The Ancient Drug Salicylate Directly Activates AMP-Activated Protein Kinase

Simon A. Hawley *et al.*

Science **336**, 918 (2012);
DOI: 10.1126/science.1215327

Science (print ISSN 0036-8075; online ISSN 1095-9203) is published weekly, except the last week in December, by the American Association for the Advancement of Science, 1200 New York Avenue NW, Washington, DC 20005.

analogous complex between YfiA and the *Eco* ribosome (*11*), as well as with 8.5 Å resolution cryo-EM density map of a similar complex between chloroplast-specific YfiA homolog, PSRP1, bound to the *Eco* ribosome (*12*). In our model, HPF and YfiA are bound in the channel that lies between the head and the body of the 30*S* subunit where tRNAs and mRNA bind during protein synthesis (Fig. 4, E and F). Although the globular domains of HPF and YfiA have overlapping binding sites, HPF stabilizes the 100*S* ribosome dimer, whereas YfiA inhibits its formation (*6*). The inhibition is due to the extended C-terminal tail of YfiA, which HPF does not have, that blocks the binding of RMF and, thus, the RMF-induced dimer formation. The visible portion of the YfiA tail follows the mRNA channel, whereas the C-terminal end of the tail, which presumably projects into the RMF binding site (Fig. 4D), could not be modeled. This observation is consistent with previous biochemical studies suggesting mutually exclusive binding of YfiA and RMF to the 70*S* ribosome (*5*). Additionally, YfiA also prevents the formation of the 100*S* dimer by stabilizing the head domain of the small subunit in its apo-conformation.

Our structures reveal that RMF and HPF can bind simultaneously and function together to interfere with the initiation of protein synthesis, which is consistent with the biochemical data (*5*). The HPF-YfiA binding site not only overlaps with all of the tRNA binding sites (Fig. 4, E and F) but also with the binding sites of the initiation factors IF1 and IF3 (fig. S6, A and B), which are directly involved in dissociation of the ribosomes into subunits (*21*), and elongation factor G (fig. S6, C and D), which assists ribosome recycling factor in dissociating posttermination complexes of 70*S* ribosomes (*22*). The inability of these factors to perform their function as a result of blocking by HPF or YfiA of their binding sites explains the reduced dissociation of the stationary-phase ribosomes into subunits (*10*). Because RMF, HPF, and YfiA bind exclusively to the 30*S* subunit, they might not only interfere with initiation of protein synthesis starting on the 70*S* ribosomes, as in the case of leaderless mRNA (*23*) or during reinitiation along polycistronic mRNAs (*24*) but also with canonical initiation starting on the 30*S* subunits.

These studies show that these stationary-phase proteins, when bound to the ribosome, sterically clash with mRNA and tRNAs, and therefore, they cannot act on actively translating ribosomes. This ensures that the stationary-phase factors function only after the completion of the ongoing translation cycles and can only act effectively during stress and/or starvation conditions when the availability of the mRNA and/or tRNAs is limiting.

References and Notes

1. A. Wada, Y. Yamazaki, N. Fujita, A. Ishihama, *Proc. Natl. Acad. Sci. U.S.A.* **87**, 2657 (1990).
2. D. E. Agafonov, V. A. Kolb, A. S. Spirin, *EMBO Rep.* **2**, 399 (2001).
3. J. L. Martinez, F. Baquero, *Antimicrob. Agents Chemother.* **44**, 1771 (2000).
4. M. Kivisaar, *Environ. Microbiol.* **5**, 814 (2003).
5. M. Ueta *et al.*, *Genes Cells* **10**, 1103 (2005).
6. M. Ueta *et al.*, *J. Biochem.* **143**, 425 (2008).
7. H. Yoshida *et al.*, *J. Biochem.* **132**, 983 (2002).
8. T. Kato *et al.*, *Structure* **18**, 719 (2010).
9. J. O. Ortiz *et al.*, *J. Cell Biol.* **190**, 613 (2010).
10. D. E. Agafonov, V. A. Kolb, I. V. Nazimov, A. S. Spirin, *Proc. Natl. Acad. Sci. U.S.A.* **96**, 12345 (1999).
11. A. Vila-Sanjurjo, B. S. Schuwirth, C. W. Hau, J. H. Cate, *Nat. Struct. Mol. Biol.* **11**, 1054 (2004).
12. M. R. Sharma *et al.*, *J. Biol. Chem.* **285**, 4006 (2010).
13. M. Selmer *et al.*, *Science* **313**, 1935 (2006).
14. Materials and methods are available as supplementary materials on *Science* Online.
15. J. Shine, L. Dalgarno, *Proc. Natl. Acad. Sci. U.S.A.* **71**, 1342 (1974).
16. J. A. Steitz, K. Jakes, *Proc. Natl. Acad. Sci. U.S.A.* **72**, 4734 (1975).
17. H. Yoshida, H. Yamamoto, T. Uchiumi, A. Wada, *Genes Cells* **9**, 271 (2004).
18. H. Jin, A. C. Kelley, V. Ramakrishnan, *Proc. Natl. Acad. Sci. U.S.A.* **108**, 15798 (2011).
19. A. Tissières, J. D. Watson, D. Schlessinger, B. R. Hollingworth, *J. Mol. Biol.* **1**, 221 (1959).
20. B. T. Wimberly *et al.*, *Nature* **407**, 327 (2000).
21. M. Y. Pavlov, A. Antoun, M. Lovmar, M. Ehrenberg, *EMBO J.* **27**, 1706 (2008).
22. L. Janosi, H. Hara, S. J. Zhang, A. Kaji, *Adv. Biophys.* **32**, 121 (1996).
23. I. Moll, G. Hirokawa, M. C. Kiel, A. Kaji, U. Bläsi, *Nucleic Acids Res.* **32**, 3354 (2004).
24. A. L. Karamyshev, Z. N. Karamysheva, T. Yamami, K. Ito, Y. Nakamura, *Biochimie* **86**, 933 (2004).
25. G. Yusupova, L. Jenner, B. Rees, D. Moras, M. Yusupov, *Nature* **444**, 391 (2006).
26. A. Rak, A. Kalinin, D. Shcherbakov, P. Bayer, *Biochem. Biophys. Res. Commun.* **299**, 710 (2002).

Acknowledgments: We thank the staff at the National Synchrotron Light Source (beamlines X29 and X25) and at the Advanced Photon Source (beamline 24ID) for help during data collection, the staff at the Center for Structural Biology at Yale University for computational support, and S. Seetharaman and M. Gagnon for valuable discussions. This work was supported by NIH grant GM022778 awarded to T.A.S. The structure factors and coordinates for both copies of the 70*S* ribosome in the asymmetric unit of all complexes have been deposited in the Research Collaboration for Structural Biology Protein Data Bank with the following accession codes: 3V22, 3V23, 3V24, and 3V25 for the RMF-ribosome complex; 3V26, 3V27, 3V28, and 3V29 for the HPF-ribosome complex; and 3V2C, 3V2D, 3V2F, and 3V2E for the YfiA-ribosome complex. T.A.S. owns stock in and is on the advisory board of Rib-X Pharmaceuticals, Inc., which does structure-based drug design targeted at the ribosome.

Supplementary Materials

www.sciencemag.org/cgi/content/full/336/6083/915/DC1
Materials and Methods
Figs. S1 to S6
Table S1
References (*27*–*41*)
Movies S1 and S2

29 December 2011; accepted 13 April 2012
10.1126/science.1218538

The Ancient Drug Salicylate Directly Activates AMP-Activated Protein Kinase

Simon A. Hawley,[1] Morgan D. Fullerton,[2] Fiona A. Ross,[1] Jonathan D. Schertzer,[2] Cyrille Chevtzoff,[1] Katherine J. Walker,[1] Mark W. Peggie,[3] Darya Zibrova,[3] Kevin A. Green,[1] Kirsty J. Mustard,[1] Bruce E. Kemp,[4] Kei Sakamoto,[3]* Gregory R. Steinberg,[2,4] D. Grahame Hardie[1]†

Salicylate, a plant product, has been in medicinal use since ancient times. More recently, it has been replaced by synthetic derivatives such as aspirin and salsalate, both of which are rapidly broken down to salicylate in vivo. At concentrations reached in plasma after administration of salsalate or of aspirin at high doses, salicylate activates adenosine monophosphate–activated protein kinase (AMPK), a central regulator of cell growth and metabolism. Salicylate binds at the same site as the synthetic activator A-769662 to cause allosteric activation and inhibition of dephosphorylation of the activating phosphorylation site, threonine-172. In AMPK knockout mice, effects of salicylate to increase fat utilization and to lower plasma fatty acids in vivo were lost. Our results suggest that AMPK activation could explain some beneficial effects of salsalate and aspirin in humans.

The medicinal effects of willow bark have been known since the time of Hippocrates. The active component is salicylate, a hormone produced by plants in response to pathogen infection (*1*). For medicinal use, it was largely replaced by aspirin (acetyl salicylate), which is rapidly broken down to salicylate in vivo (*2*, *3*). Salicylate can also be administered as salsalate, which shows promise for treatment of insulin resistance and type 2 diabetes (*4*, *5*). Aspirin and salicylate inhibit cyclo-oxygenases and, hence, prostanoid biosynthesis (*6*), as well as the protein kinase IκB kinase β (IKKβ) in the NF-κB pathway (*7*). However, some effects of these drugs are still observed in mice deficient in these pathways (*8*).

Adenosine monophosphate–activated protein kinase (AMPK) is a cellular energy sensor con-

[1]Division of Cell Signalling and Immunology, College of Life Sciences, University of Dundee, Dundee DD1 5EH, Scotland, UK. [2]Divisions of Endocrinology and Metabolism, Department of Medicine, and Department of Biochemistry and Biomedical Sciences, McMaster University, 1200 Main Street West, Hamilton, Ontario L8N 3Z5, Canada. [3]Medical Research Council Protein Phosphorylation Unit, College of Life Sciences, University of Dundee, Dundee DD1 5EH, Scotland, UK. [4]St. Vincent's Institute of Medical Research and Department of Medicine, University of Melbourne, 41 Victoria Parade, Fitzroy, Vic 3065 Australia.

*Present address: Nestlé Institute of Health Sciences Société Anonyme, Campus École Polytechnique Fédérale de Lausanne, 1015 Lausanne, Switzerland.

†To whom correspondence should be addressed: E-mail: d.g.hardie@dundee.ac.uk

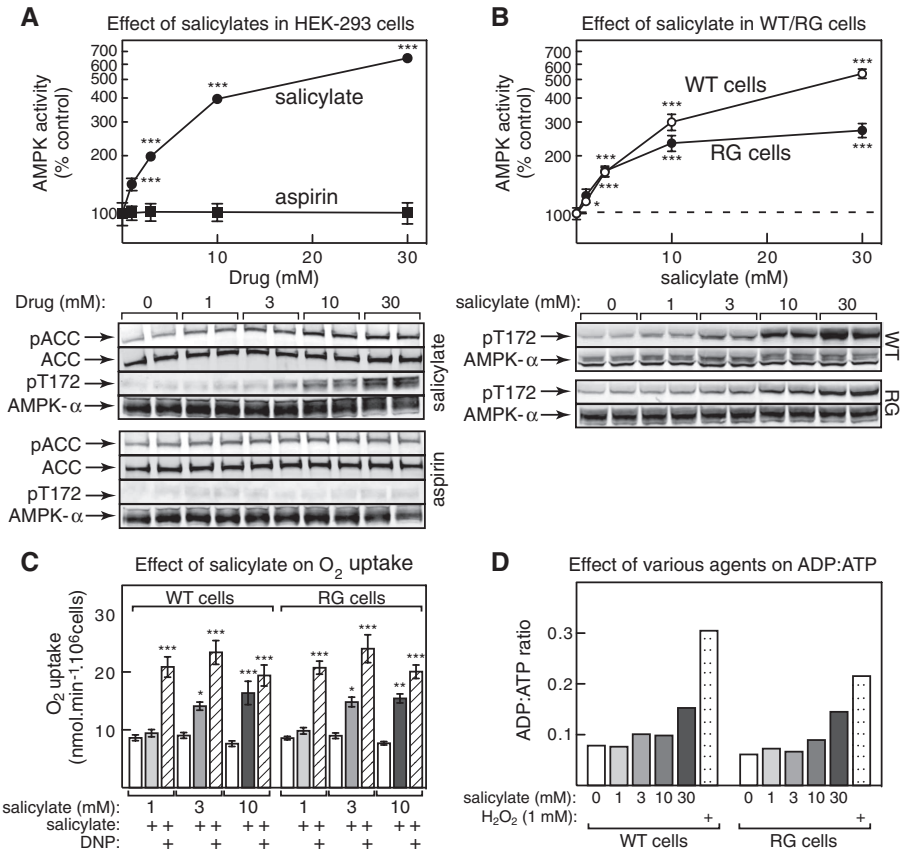

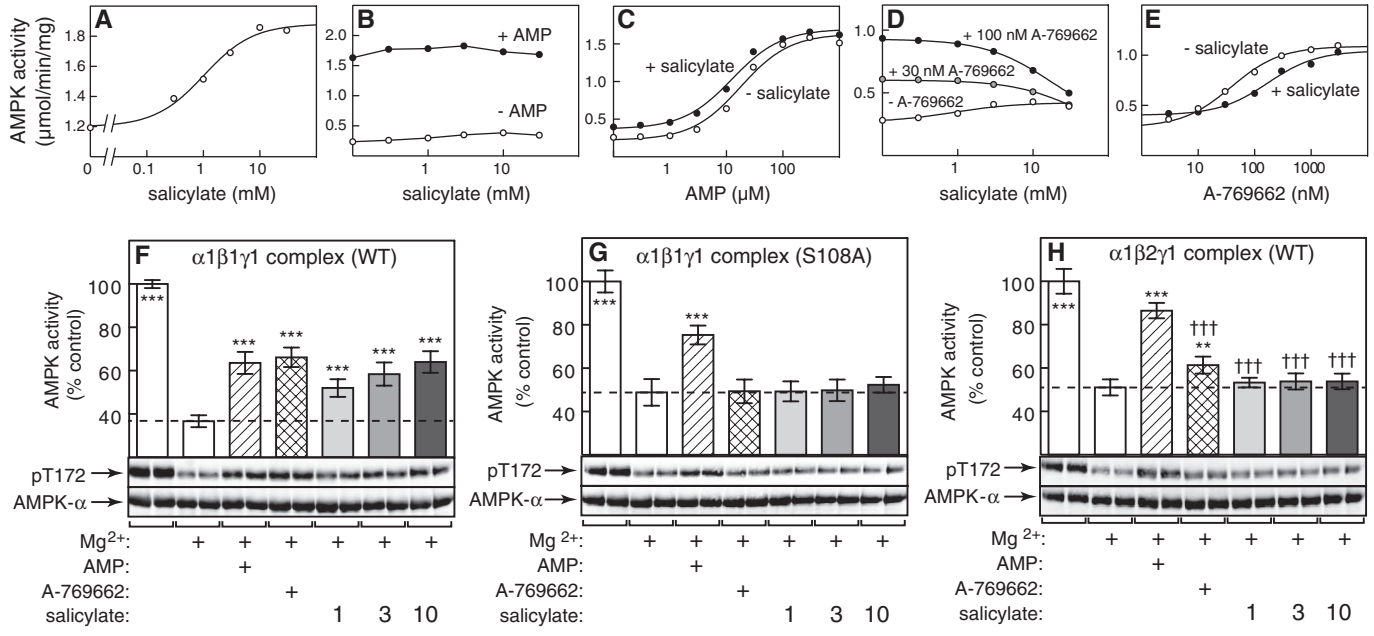

Fig. 1. Effects of salicylate in HEK-293 cells. (**A**) Effects of salicylate or aspirin on AMPK activity [mean ± SD (error bars), $n = 4$ wells of cells] and phosphorylation of AMPK (Thr^{172}) and ACC (Ser^{79}) ($n = 2$). (**B**) Effects of salicylate on AMPK activity (mean ± SD, $n = 6$) and phosphorylation ($n = 2$) in HEK-293 cells stably expressing WT γ2 or an R531G substitution (RG). In (A) and (B), the activity is plotted on a logarithmic scale as percentage of control without drug, and effects significantly different from control without drug [two-way analysis of variance (ANOVA), with Bonferroni's test comparing each drug concentration to control without drug) are shown (*$P < 0.05$, ***$P < 0.001$). (**C**) Effect of salicylate on oxygen uptake in WT and RG cells [mean ± SD, $n = 7$ to 13; significant differences by two-way ANOVA, using Bonferroni's test to compare with basal values without salicylate or 2,4-dintrophenol (DNP)] are shown (*$P < 0.05$, **$P < 0.01$, ***$P < 0.001$). (**D**) Effects of salicylate or H_2O_2 (1 mM) on ADP:ATP ratios (means of duplicate cell incubations) are shown.

Fig. 2. Effect of salicylate on AMPK in cell-free assays. (**A** to **E**) Effects of salicylate on activity of purified rat liver AMPK: (A) effect of salicylate, (B) effect of salicylate ± 200 μM AMP, (C) effect of AMP ± 10 mM salicylate, (D) effect of salicylate ± 30 and 100 nM A-769662, and (E) effect of A-769662 ± 10 mM salicylate. Data points in (A) to (E) are means of duplicate assays; lines were generated by fitting data to the equation: activity = basal + [basal*(activation − basal)*X/($A_{0.5}$ + X)], where X is the concentration of the activator. Values obtained for $A_{0.5}$ and activation are quoted in the text. (**F** to **H**) Effects of AMP, A-769662, and salicylate on dephosphorylation of bacterially expressed human AMPK complexes by PP2Cα (all incubations contained PP2Cα, but control lacked Mg^{2+}); bar graphs show AMPK activity (percentage of control without Mg^{2+}, mean ± SD, $n = 6$); gel pictures show Thr^{172} phosphorylation ($n = 2$). (F) WT α1β1γ1 complex, (G) α1β1γ1 complex with β1 S108A substitution, and (H) WT α1β2γ1 complex. Significant differences from the control plus Mg^{2+}, using one-way ANOVA with Dunnett's multiple comparison test, are shown: **$P < 0.01$, ***$P < 0.001$. Also shown are significant differences in the size of the effect of A-76962 or salicylate between the α1β1γ1 and α1β2γ1 complexes (2F and 2H): †††$P < 0.001$. For the latter comparisons, the differences between the $+Mg^{2+}$+A-76922 or $+Mg^{2+}$ +salicylate and the $+Mg^{2+}$ only columns were first expressed as a fraction of the difference between the $+Mg^{2+}$+AMP and $+Mg^{2+}$ only columns.

served throughout eukaryotes. This heterotrimeric enzyme is composed of catalytic α subunits and regulatory β and γ subunits (*9*, *10*). Once activated in response to metabolic stress, AMPK phosphorylates targets that switch off adenosine triphosphate (ATP)–consuming processes while switching on catabolic pathways that generate ATP. AMPK is activated >100-fold by phosphorylation at Thr^{172} in the α subunit by the tumor suppressor protein kinase, LKB1, or the Ca^{2+}-dependent kinase, CaMKKβ (calmodulin-dependent kinase kinase-β) (*9*, *10*). Binding of AMP or adenosine diphosphate (ADP) to the γ subunit triggers a conformational change that promotes phosphorylation and inhibits dephosphorylation (*11*–*15*), causing a switch to the active form. Binding of AMP (but not ADP) to a second site (*15*) causes further allosteric activation, leading to >1000-fold activation overall (*16*). Most drugs or xenobiotics that activate AMPK work by inhibiting mitochondrial ATP synthesis and increasing the concentration of AMP and ADP (*17*). However, a synthetic activator, A-769662 (*18*), which also causes allosteric activation and inhibits Thr^{172} dephosphorylation, binds directly to AMPK at sites distinct from those used by AMP (*19*–*21*).

Salicylate, but not aspirin, activated AMPK when applied to human embryonic kidney (HEK) 293 cells, with its effects being significant at 1 mM and above (Fig. 1A; it appears that the esterases that catalyze breakdown of aspirin to salicylate are not expressed in these cells). This was associated with increased phosphorylation of Thr^{172} on AMPK-α and the downstream target of AMPK, acetyl–coenzyme A carboxylase (ACC); in the latter case, the effects were evident at 1 mM and above (Fig. 1A). Salicylate can uncouple mitochondrial respiration (*22*), so we suspected that it might activate AMPK by decreasing cellular ATP and increasing AMP and ADP. To test this, we used isogenic cell lines expressing wild-type AMPK (WT cells) or a mutated enzyme in which an Arg^{531}→Gly^{531} (R531G) substitution in γ2 renders AMPK insensitive to AMP or ADP (RG cells) (see supplemental materials and methods) (*15*, *17*). At concentrations <10 mM, salicylate caused similar increases in AMPK phosphorylation or activation in WT and RG cells, showing that the effect was not dependent on changes in AMP or ADP. However, at 10 mM and above, there was a greater activation/phosphorylation in WT than in RG cells, suggesting that AMP- or ADP-dependent effects were also occurring at these higher concentrations (Fig. 1B). Concentrations >1 mM salicylate increased cellular oxygen uptake in both WT and RG cells. This effect was not additive with the effect of a concentration of dinitrophenol causing a maximal increase in oxygen uptake, suggesting that at these concentrations, salicylate, like dinitrophenol, could dissipate the proton gradient and thus uncouple the respiratory chain from ATP synthesis (Fig. 1C). However, unlike effects of another AMPK activator (H_2O_2), any increases in the cellular ADP:ATP ratio at salicylate concentrations below 30 mM were very small (Fig. 1D). Thus, mitochondria appear to compensate for mild uncoupling by increasing respiration. Salicylate does not activate AMPK through the Ca^{2+}-CaMKKβ pathway (*12*), because the CaMKK inhibitor STO-609 had no effect on responses to salicylate, although it blocked responses to a Ca^{2+} ionophore, A23187 (fig. S1, A and B, supplementary data).

Using a physiological concentration of ATP in assays (2 mM), salicylate caused a 1.6-fold allosteric activation with a half-maximal effect ($A_{0.5}$) at 1.0 ± 0.2 mM (Fig. 2A). We observed a large activation by AMP at all salicylate concentrations

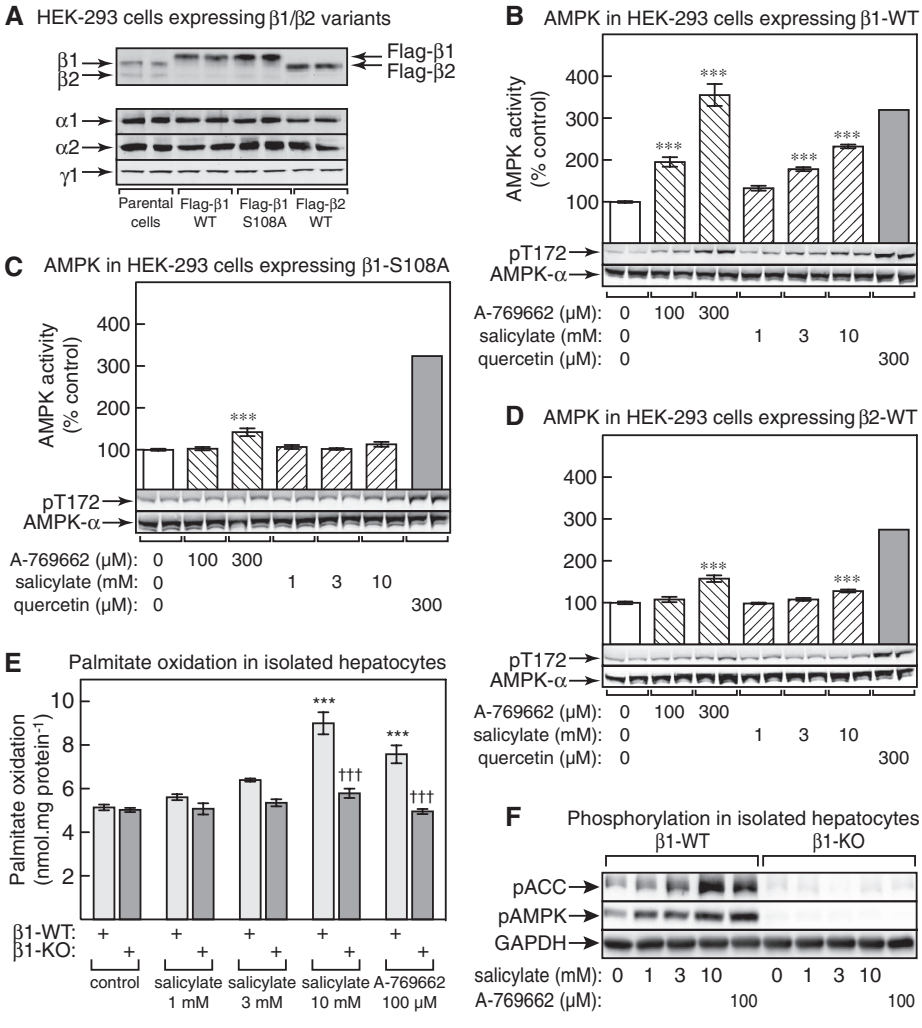

Fig. 3. Effects of salicylate and A-769662 in intact cells. (**A**) Expression of β subunits assessed using pan-β antibody in parental cells or cells stably expressing β1 WT, β1-S108A, or β2 WT and of endogenous α1, α2, and γ1 in the same cells. (**B** to **D**) Activity and phosphorylation of AMPK after treatment with various activators in cells expressing (B) β1 WT, (C) β1-S108A, and (D) β2 WT. Kinase assays [mean ± SEM, $n = 6$ except for 100 μM A-769662 ($n = 4$) and quercetin ($n = 2$); significantly different from control without drug, by one-way ANOVA with Dunnett's multiple comparison test, ***$P < 0.001$] and Western blots ($n = 2$) were of immunoprecipitates made using an antibody to FLAG. (**E**) Palmitate oxidation in hepatocytes isolated from β1-KO mice and WT controls (mean ± SEM, $n = 6$ to 14, significantly different from control without drug by two-way ANOVA with Bonferroni's test, ***$P < 0.001$; †††significantly different from WT, $P < 0.001$). (**F**) Phosphorylation of AMPK and ACC in hepatocytes isolated from β1-KO or WT mice. GAPDH, glyceraldehyde-3-phosphate dehydrogenase.

up to 30 mM (Fig. 2B), and salicylate did not affect the concentration of AMP causing half-maximal activation ($A_{0.5}$ = 18 ± 3 or 13 ± 2 μM, with or without 10 mM salicylate) (Fig. 2C). In contrast, increasing concentrations of salicylate progressively antagonized activation by 30 and 100 nM A-769662 (Fig. 2D), and 10 mM salicylate increased $A_{0.5}$ for A-769662 by >fourfold (from 39 ± 4 to 172 ± 24 nM) (Fig. 2E). These results suggest that salicylate is a partial agonist acting at the same site as A-769662, causing a small activation on its own but antagonizing the larger activation by A-769662. If it binds at the same site, salicylate should protect against Thr^{172} dephosphorylation, as does A-769662 (*19*, *20*). Indeed, salicylate protected AMPK (human α1β1γ1 complex) against dephosphorylation and inactivation by protein phosphatase-2Cα to the same extent as did AMP and A-769662 (Fig. 2F), although it had no effect on PP2Cα assayed using a peptide substrate (fig. S2). A Ser^{108}→Ala^{108} (S108A) substitution in the β1 subunit abolishes effects of A-769662 on dephosphorylation, and β2-containing complexes are resistant to the drug (*20*, *21*). As expected, an S108A substitution in the α1β1γ1 complex abolished the effects of A-769662 and salicylate, but not that of AMP (Fig. 2G), whereas there was no effect of salicylate on dephosphorylation of an α1β2γ1 complex, although there was a small effect of A-769662 (Fig. 2H). These results lend further support to the idea that salicylate binds at the same site(s) as A-769662.

To examine effects of salicylate on AMPK phosphorylation and activation in intact cells, we used HEK-293 cells carrying a Flp recombinase target site to generate isogenic lines expressing FLAG-tagged WT β1, a β1-S108A mutant, or WT β2. With the use of an antibody that recognizes both isoforms, endogenous β1 and β2 could be detected in the parental cells, but, as observed previously when expressing α subunits using this system (*17*), these were largely replaced by FLAG-tagged β1 and β2 (with reduced electrophoretic mobility) in cells expressing recombinant β1/β2; the expression of α1, α2, and γ1 subunits was unaffected (Fig. 3A). A-769662 and salicylate caused increased activation/phosphorylation of AMPK in cells expressing WT β1 (Fig. 3B), but their effects were greatly reduced in cells expressing the β1-S108A mutant (Fig. 3C) or WT β2 (Fig. 3D), In contrast, the effects of quercetin, which acts by increasing AMP (*17*), were unaffected.

We used β1 knockout (KO) mice to test whether salicylate has metabolic effects in vivo through AMPK (*23*). Fatty-acid oxidation in isolated WT hepatocytes was stimulated by salicylate or A-769662 and was associated with increased phosphorylation of AMPK and ACC [the latter regulating fat oxidation (*24*)]. All effects were reduced or eliminated in hepatocytes from β1-KOs (Fig. 3, E and F, and fig. S3). There were no changes in ADP:ATP ratios in WT cells in response to 1 to 10 mM salicylate (fig. S4A).

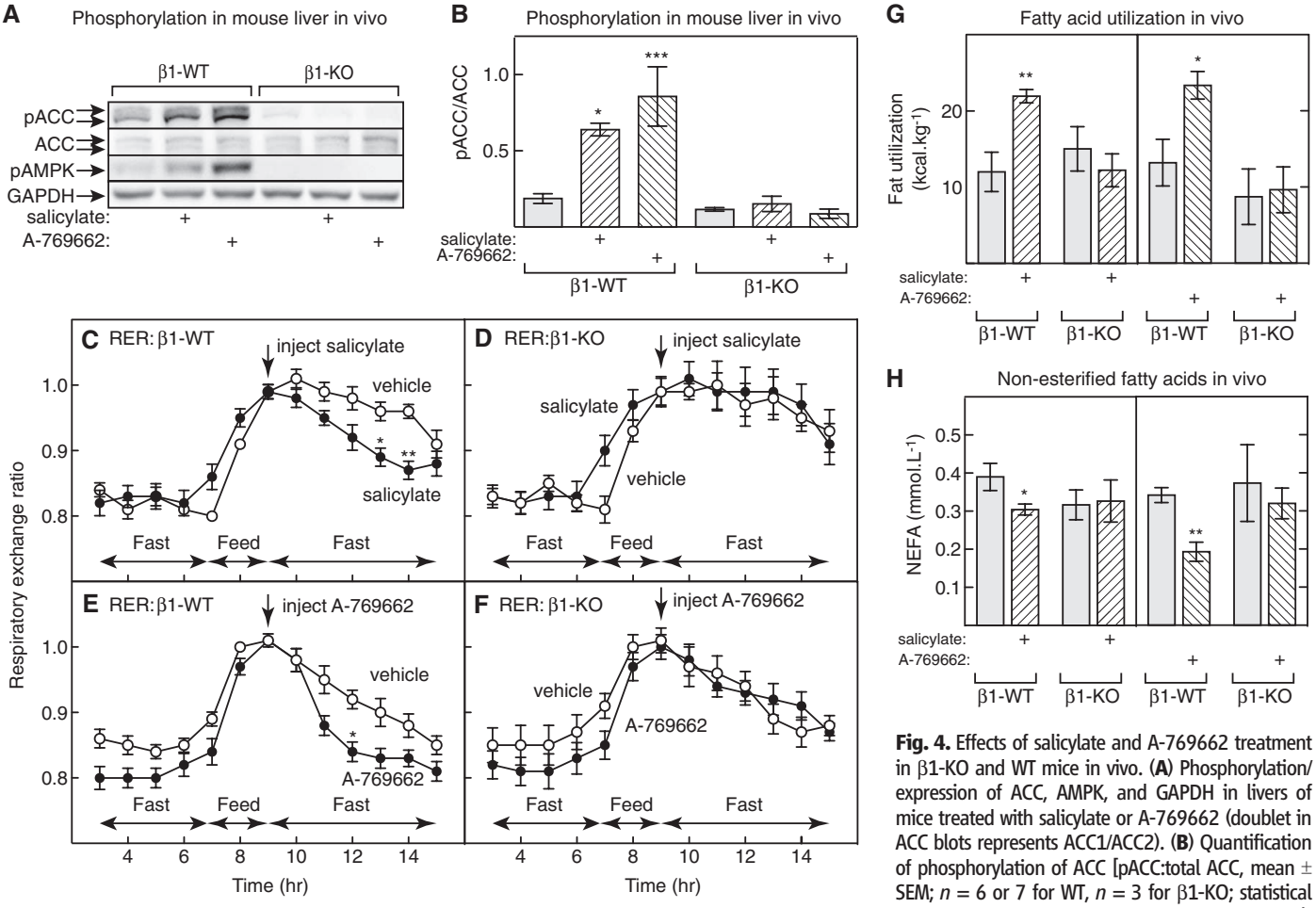

Fig. 4. Effects of salicylate and A-769662 treatment in β1-KO and WT mice in vivo. (**A**) Phosphorylation/expression of ACC, AMPK, and GAPDH in livers of mice treated with salicylate or A-769662 (doublet in ACC blots represents ACC1/ACC2). (**B**) Quantification of phosphorylation of ACC [pACC:total ACC, mean ± SEM; n = 6 or 7 for WT, n = 3 for β1-KO; statistical significance by one-way ANOVA with Bonferroni's test compared with vehicle only is shown (*P < 0.05, ***P < 0.001)]. (**C** to **F**) RER measured in β1-KO and WT mice after injection of vehicle, salicylate (250 mg/kg), or A-769662 (30 mg/kg) at the start of a period of fasting. Results are mean ± SEM (n = 6 to 13). By two-way ANOVA, effects of salicylate (P < 0.05) or A-769662 (P < 0.001) were only significant in WT mice; significant differences by Bonferroni's test at individual time points are shown (*P < 0.05, **P < 0.01). (**G**) Fatty-acid utilization calculated from data in (C) to (F). Results are mean ± SEM (n = 7 or 8). Significant differences by two-way ANOVA with Bonferroni's test are shown (*P < 0.05, **P < 0.01). (**H**) Plasma nonesterified fatty acids (NEFA) in mice treated with salicylate or A-769662 for 90 min. Results are mean ± SEM (n = 7 or 8). Significant differences by two-way ANOVA with Bonferroni's test are shown (*P < 0.05, **P < 0.01).

We injected mice with salicylate or A-769662 at the start of a period of fasting to assess metabolism in vivo. The dose that we used generated plasma salicylate of 2.4 ± 0.4 and 2.0 ± 0.1 mM (mean ± SEM, $n = 7$ and 3 mice) in WT and β1-KO mice, respectively. Both agents caused phosphorylation of liver AMPK and ACC in WT but not β1-KO mice (Fig. 4, A and B), although there were no changes in hepatic AMP:ATP or ADP:ATP ratios in WT mice (fig. S4B). In WT mice, salicylate also caused phosphorylation and activation of AMPK in soleus muscle and adipose tissue (fig. S5). Both agents depressed the respiratory exchange ratio (RER) for 6 hours after injection, consistent with a switch from carbohydrate to fat utilization; these effects were lost in β1-KOs (Fig. 4, C to F). Significant depressions in RER, in WT mice only, were evident by calculating the area under the curve (fig. S6, A and B). When we calculated fat and carbohydrate utilization, both salicylate and A-769662 increased fat utilization in WT but not β1-KO mice (Fig. 4G); A-769662 also decreased carbohydrate utilization in WT mice (fig. S6, C and D). Both salicylate and A-769662 reduced serum nonesterified fatty acids in WT but not β1-KO mice (Fig. 4H). We also studied glucose homeostasis in mice made insulin-resistant by high-fat feeding, followed by daily salicylate injections for 2 weeks. However, effects of salicylate to improve fasting glucose, fasting insulin, glucose tolerance, and insulin resistance (homeostasis model assessment) were retained in β1-KO mice (fig. S7), indicating that they were independent of AMPK.

Our results show that salicylate can directly activate AMPK, primarily by inhibiting Thr^{172} dephosphorylation. The plasma salicylate concentrations in humans treated with oral salsalate (*4*) or high-dose aspirin (30 to 90 mg/kg) (*25*, *26*) are 1 to 3 mM. At these concentrations, salicylate activated AMPK in WT and RG HEK-293 cells to the same extent and did not increase cellular ADP:ATP ratios, indicating an AMP-independent mechanism. Thus, the natural product salicylate can activate AMPK via a mechanism closely related to that of A-769662, a synthetic activator derived from a high-throughput screen [which, unlike salicylates, has poor oral availability (*18*)]. Although the exact site(s) occupied by salicylate and A-769662 on AMPK remain unidentified, our finding that the S108A mutation abolishes activation by both agents suggests that the binding sites overlap.

Effects of salicylate on fat oxidation in vivo appear to require activation of AMPK-β1 complexes. Aspirin also reduces circulating lipids in obese rats and improves insulin sensitivity (*7*). However, in agreement with previous studies (*7*, *27*), our results using long-term salicylate treatment of fat-fed mice (fig. S7) indicate that effects on AMPK-independent pathways, such as IKKβ or c-Jun N-terminal kinase, are also important.

After oral administration, aspirin is rapidly broken down by liver, erythrocyte, and plasma esterases to salicylate (*3*), whose peak plasma concentrations and half-life are orders of magnitude greater than those of aspirin (*2*). Our findings raise the possibility that other effects of aspirin, like protective effects against development of cancer (*28*), may be mediated in part by AMPK. AMPK is activated by the antidiabetic drug metformin (*17*, *29*), and treatment of diabetics with metformin is also associated with reduced cancer incidence (*30*). Our results show that one thing salicylates and metformin have in common is their ability to activate AMPK. However, one caveat is that the doses of aspirin required to activate AMPK in vivo may be higher than those used in most human studies.

Note added in proof: While this paper was being reviewed, Din *et al.* [F. V. N. Din *et al.*, *Gastroenterology* 10.1053/j.gastro.2012.02.050 (2012)] reported that aspirin activates AMPK in colorectal cancer cell lines.

References and Notes

1. P. Reymond, E. E. Farmer, *Curr. Opin. Plant Biol.* **1**, 404 (1998).
2. G. A. Higgs, J. A. Salmon, B. Henderson, J. R. Vane, *Proc. Natl. Acad. Sci. U.S.A.* **84**, 1417 (1987).
3. F. M. Williams, *Clin. Pharmacokinet.* **10**, 392 (1985).
4. A. Fleischman, S. E. Shoelson, R. Bernier, A. B. Goldfine, *Diabetes Care* **31**, 289 (2008).
5. A. B. Goldfine *et al.*, *Ann. Intern. Med.* **152**, 346 (2010).
6. G. A. Higgs, S. Moncada, J. R. Vane, *Ann. Clin. Res.* **16**, 287 (1984).
7. M. Yuan *et al.*, *Science* **293**, 1673 (2001).
8. B. N. Cronstein, M. C. Montesinos, G. Weissmann, *Proc. Natl. Acad. Sci. U.S.A.* **96**, 6377 (1999).
9. D. G. Hardie, *Nat. Rev. Mol. Cell Biol.* **8**, 774 (2007).
10. G. R. Steinberg, B. E. Kemp, *Physiol. Rev.* **89**, 1025 (2009).
11. J. S. Oakhill *et al.*, *Science* **332**, 1433 (2011).
12. S. A. Hawley *et al.*, *J. Biol. Chem.* **270**, 27186 (1995).
13. J. S. Oakhill *et al.*, *Proc. Natl. Acad. Sci. U.S.A.* **107**, 19237 (2010).
14. S. P. Davies, N. R. Helps, P. T. W. Cohen, D. G. Hardie, *FEBS Lett.* **377**, 421 (1995).
15. B. Xiao *et al.*, *Nature* **472**, 230 (2011).
16. M. Suter *et al.*, *J. Biol. Chem.* **281**, 32207 (2006).
17. S. A. Hawley *et al.*, *Cell Metab.* **11**, 554 (2010).
18. B. Cool *et al.*, *Cell Metab.* **3**, 403 (2006).
19. O. Göransson *et al.*, *J. Biol. Chem.* **282**, 32549 (2007).
20. M. J. Sanders *et al.*, *J. Biol. Chem.* **282**, 32539 (2007).
21. J. W. Scott *et al.*, *Chem. Biol.* **15**, 1220 (2008).
22. T. M. Brody, *J. Pharmacol. Exp. Ther.* **117**, 39 (1956).
23. N. Dzamko *et al.*, *J. Biol. Chem.* **285**, 115 (2010).
24. L. Abu-Elheiga, M. M. Matzuk, K. A. H. Abo-Hashema, S. J. Wakil, *Science* **291**, 2613 (2001).
25. R. O. Day *et al.*, *Br. J. Clin. Pharmacol.* **28**, 695 (1989).
26. R. S. Hundal *et al.*, *J. Clin. Invest.* **109**, 1321 (2002).
27. Z. Gao, A. Zuberi, M. J. Quon, Z. Dong, J. Ye, *J. Biol. Chem.* **278**, 24944 (2003).
28. P. M. Rothwell *et al.*, *Lancet* **377**, 31 (2011).
29. G. Zhou *et al.*, *J. Clin. Invest.* **108**, 1167 (2001).
30. A. A. Ogunleye, S. A. Ogston, A. D. Morris, J. M. Evans, *Br. J. Cancer* **101**, 1199 (2009).

Acknowledgments: D.G.H. was supported by a Programme Grant (080982) from the Wellcome Trust and K.S. by the Medical Research Council. D.G.H. and K.S. were also funded by the companies (AstraZeneca, Boehringer-Ingelheim, GlaxoSmithKline, Merck Serono, and Pfizer) supporting the Division of Signal Transduction Therapy, Univ. of Dundee. The studies were also supported by grants and fellowship from the Canadian Institutes of Health Research (CIHR) (M.D.F. and G.R.S.), the Canadian Diabetes Association (J.D.S. and G.R.S.), the National Health and Medical Research Council of Australia (G.R.S. and B.E.K.), and the Australian Research Council and the Victorian Government's Operational Infrastructure Support Program (B.E.K.). J.D.S. is a DeGroote Academic Fellow (McMaster Univ.), and M.D.F. a Banting Postdoctoral Fellow (CIHR). G.R.S. is a Canada Research Chair in Metabolism and Obesity.

Supplementary Materials

www.sciencemag.org/cgi/content/full/science.1215327/DC1
Materials and Methods
Figs. S1 to S7
References

17 October 2011; accepted 23 March 2012
Published online 19 April 2012;
10.1126/science.1215327

Aerobic Microbial Respiration in 86-Million-Year-Old Deep-Sea Red Clay

Hans Røy,[1]* Jens Kallmeyer,[2] Rishi Ram Adhikari,[2] Robert Pockalny,[3] Bo Barker Jørgensen,[1] Steven D'Hondt[3]

Microbial communities can subsist at depth in marine sediments without fresh supply of organic matter for millions of years. At threshold sedimentation rates of 1 millimeter per 1000 years, the low rates of microbial community metabolism in the North Pacific Gyre allow sediments to remain oxygenated tens of meters below the sea floor. We found that the oxygen respiration rates dropped from 10 micromoles of O_2 $liter^{-1}$ $year^{-1}$ near the sediment-water interface to 0.001 micromoles of O_2 $liter^{-1}$ $year^{-1}$ at 30-meter depth within 86 million-year-old sediment. The cell-specific respiration rate decreased with depth but stabilized at around 10^{-3} femtomoles of O_2 $cell^{-1}$ day^{-1} 10 meters below the seafloor. This result indicated that the community size is controlled by the rate of carbon oxidation and thereby by the low available energy flux.

The discovery of living microbial communities in deeply buried marine sediments (*1*, *2*) has spurred interest in life under extreme energy limitation (*3*). The subtropical gyres are the most oligotrophic regions of the oceans. Primary productivity in the surface waters of the gyres is low, yet within the same order of magnitude as the surrounding open ocean (Fig. 1). Oxygen penetrates many meters into the seabed below the gyres, which indicates extremely low rates of microbial community respiration (*4*, *5*) in contrast to the rest of the seabed